A Very High Density Floating Electrode Flexible Sensor Array for High-Resolution Measurements of Contact Forces

Rajesh Surapaneni, Qingbo Guo, Darrin J. Young and Carlos H. Mastrangelo
Electrical and Computer Engineering
University of Utah
Salt Lake City, UT, USA
Rajesh.surapaneni@utah.edu

***Abstract*— We present the development, fabrication and testing results of a new high-density flexible sensor array (HDFA) suitable of recording three-axis stresses with high spatial resolution. The new HDFA consists of 676 (26×26) sensing cells fabricated on top of a high-density flex circuit substrate. Each sensing cell is implemented using four floating comb electrodes separated from the flex substrate by a thin layer of a compressible PDMS film. Each sensing cell measures 2.77×2.55 mm^2 thus packing 2704 capacitors in an area of ~ 50 cm^2. The HDFA is read using a high-speed switched-capacitor circuit with a 13-bit resolution at full frame rates of 100 Hz (~0.8Mb/s). The new array is capable of detecting contact line displacements as low as 35 µm and contact line velocities as low as 38 µm/s.**

I. Introduction

Flexible mechanical sensors that are able to measure contact forces and withstand many large deformation cycles are needed in diverse applications including robotic grippers, wearable sensor systems, impact and contact sensors [1]. These sensors are generally difficult to produce because of periodic deformation breaks metal interconnects after just a few hundreds or thousands of cycles. The introduction of floating electrodes in the sensing cells [2-3] has significantly improved the sensor reliability as the floating electrodes are well known to be immune to the presence of the metal breaks. Floating electrodes were recently used to implement 8×8 array imagers that indirectly map pressure and shear [4]. Recently, we have developed a 13×13 array of sensing cells with floating electrodes that measure both pressure and two dimensional shear simultaneously [5]. In this paper, we report the fabrication of a 26×26 array. The array occupies roughly the same area as that of our previous design but the target cell capacitance is approximately the same. Accomplishing this requires careful scaling of the cell dimensions as well as minimization of nominal capacitance mismatches caused by wire routing fringing and feed through capacitances. Additional details about multiplexing schemes and the readout circuitry for these devices are discussed in references [5-6].

This project has been sponsored under DARPA Contract W31P4Q-08-C-0253.

II. HDFA Cell with Reduced Feedthrough

Each sensing cell consists of an X-cell and a Y-cell. Together they are capable of measuring normal stress and two dimensional shear stress. Fig. 1 shows a cross section of an example X-cell. The cell consists of a series of interdigitated finger electrodes placed at two different heights separated by an elastic dielectric film. The drive and the sense electrodes are placed at the same height and next to each other. The

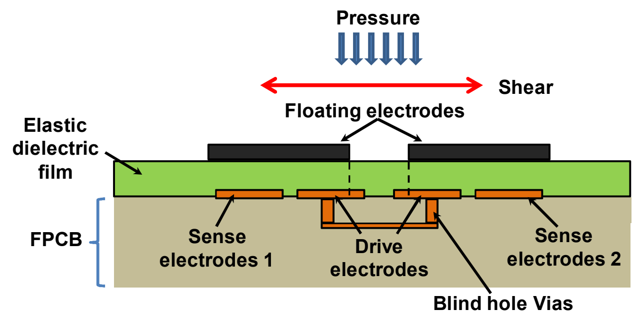

Figure 1. Cross-sectional schematic of a sensing cell. The floating electrodes are placed with an offset with respect to the drive electrodes to enable the pressure and shear measurement capabilities.

sense electrodes in a column are connected together while the drive electrodes in a row are connected together using via holes. The floating electrodes overlap completely over the sense electrodes while maintaining an offset on the drive electrodes. This offset in overlap provides the shear signal. When normal forces alone are acting on the floating electrode, capacitance increases equally on all four capacitors of the sensing cell. When shear is applied in addition to normal load, capacitances increase or decrease depending on the direction of shear.

The pressure and shear sensitivities of the cell structure are given by Eqs. (1)-(3), respectively,

978-1-4673-4642-9/13/$31.00 ©2013 IEEE

$$S_P^F = \frac{1}{E} \quad (1)$$

$$S_{SX}^F = \frac{N_{fx} \cdot t}{2 \cdot G \cdot w_f} \quad (2)$$

$$S_{SY}^F = \frac{N_{fy} \cdot t}{G \cdot w_f} \quad (3)$$

where E and G are the elastic and shear modulus of the deformable dielectric, t is dielectric thickness, w_f is the finger width and N_{fx} and N_{fy} are the number of floating electrodes in the corresponding half cells. The shear sensitivity of this design thus increases linearly with the number of fingers.

a) HDFA Cell Scaling: In order to scale down the cell size while maintaining a comparable signal range we examined carefully the effects of routing fringing field and feed through capacitances. Fig. 2 shows a comparison of the cells from our 13×13 and the new 26×26 arrays. In the older cell, shown in Fig. 2(a), the cell area was minimized, but the capacitance contribution of the routing wires was ignored. The most compact layout utilized a drive line that was in close proximity (100 µm) to a parallel sense line for the X-cell for a significant distance, approximately 80% of the cell width. This resulted on a larger signal from the X-cell than that observed in the Y-cell, even though they both have identical overlap and edge distances. The increased readout signal of the X-cell (~0.9 V) effectively reduced the dynamic range of the array readout circuit that had a full range of 3V.

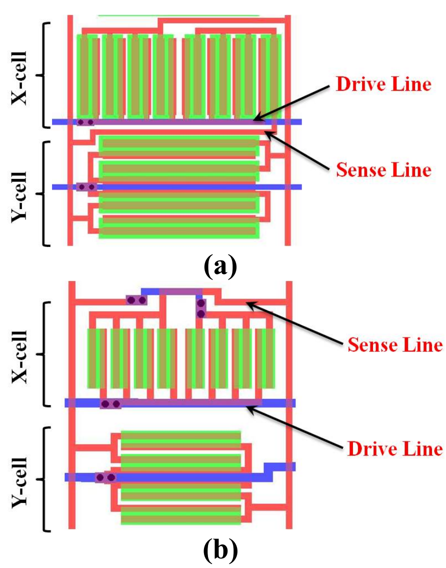

Figure 2. (a) Sensing cell of previous design with drive and the sense lines close to each other causing fringing capacitance feed through (crowded electrical interconnects), (b) new design with sense and drive lines separated from each other.

The new array cell separates the drive and the sense lines from each other as shown in Fig. 2(b) by 950 µm and remains 300 µm away from the Y-cell top sense line. This separation increase helped to reduce the output signal variation between the X and Y-cells significantly improving the dynamic range. We performed a finite element analysis on this new design also verified the nominal capacitances of X-cell and Y-cell matching each other within 0.1 pF from each other.

. The nominal capacitance of the older cell design [5] was 1.1 pF. The elastic dielectric gap between the floating electrodes and the drive/sense electrodes in the older cell was 40 µm (15 µm PDMS and 25 µm polyimide). In order to maintain a similar cell capacitance, the new HDFA cell incorporates a single layer of PDMS (10 µm thick). The reduced dielectric thickness compensates for the smaller cell size. The HDFA sensing cell shown in Fig. 3 measures 2.77×2.55 mm^2, packing 2704 capacitors in an area of ~50 cm^2. Each floating electrode is 700 µm and the overlap area with respect to the drive and sense electrodes is 0.28 mm^2 and 0.42 mm^2 respectively. Using a 10 µm thick polydimethylsiloxane (PDMS) elastic dielectric material of dielectric constant 2.8, the calculated nominal cell capacitance in each of X-cell and Y-cell is ~0.84 pF. The finite element simulation showed a nominal capacitance of ~0.77 pF in close agreement.

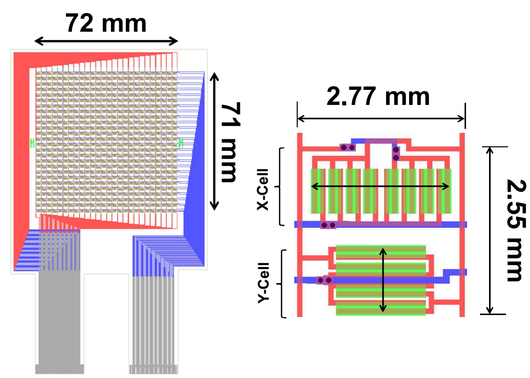

Figure 3. Layout design of the entire HDFA. The sensing cell with X-cell and Y-cell measuring shear in the direction represented by the arrows.

III. Fabrication

The HDFAs are fabricated using flexible printed circuit board (FPCB) techniques and post-processing with microfabrication techniques for deposition of floating electrodes on elastic dielectric material (PDMS). Employing FPCB substrates assure a high manufacturing yield and construct devices of any dimensions/shapes with built-in connector cables.

Fig. 4 shows a simplified fabrication process flow. A custom two-layer FPCB substrate is fabricated with the desired sense and drive electrodes patterned using the layout file shown in Fig. 3. The FPCB substrates are fabricated elsewhere (Microconnex, USA) with a minimum line width of 75 µm using the following process steps. A flexible 25µm Kapton base panel with 4 µm copper (Cu) is hard rolled with dry photoresist and patterned to form the image of the designed layout. After etching unwanted copper, drive and sense lines are formed. Via holes are formed on the Kapton layer to connect the drive electrodes on the same row together. A second layer of 4 µm Cu is deposited using sputtering technique and patterned using dry photoresist. This patterned layer of Cu connects the via holes in the same row. This Cu is protected by adhering a coverlay material (similar to Kapton film). The electrical connections from drive and sense electrodes are patterned such that they form a flat flex cable that can be connected to the readout circuit board using a low profile flip-lock connector. This stack of layers form the FPCB substrate.

Next, a 10 µm thick PDMS layer is spin-coated to form the elastic dielectric material. Fig. 5 shows the curve of PDMS thickness versus spin time (Sylgard 184, Dow Corning, USA, 10:1 polymer to curing agent ratio) at 2000 rpm after a 65°C overnight cure. A thickness of 10 µm is achieved by spinning PDMS at 2000 rpm for 10 minutes. This PDMS layer is deposited directly on the drive and sense electrodes. Next, a 50 nm Cr and 100 nm Au thin films are deposited by e-beam evaporator. The films are next patterned to form the floating electrodes. Fig. 6 shows photographs of the fabricated HDFA.

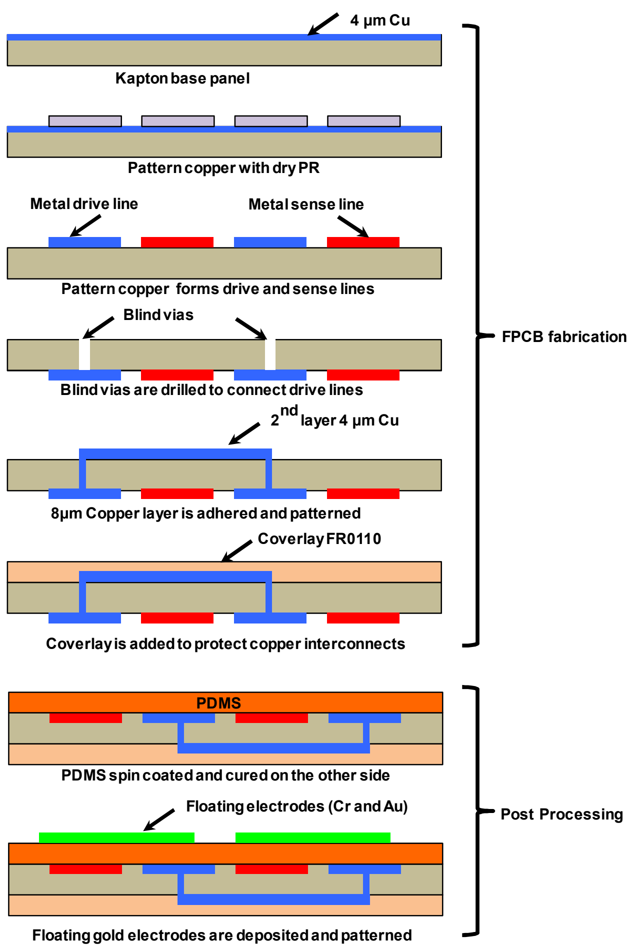

Figure 4. Process flow representing FPCB fabrication and post processing. Post-processing involves PDMS layer spin-coating and deposition and patterning of thin film metallization to form the floating electrodes.

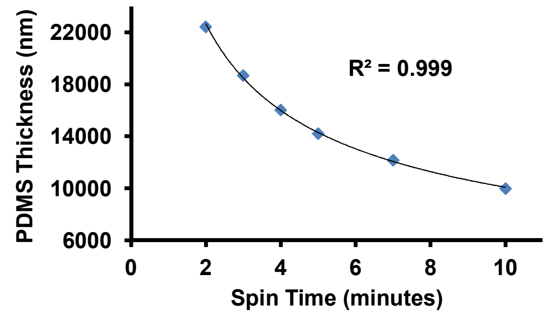

Figure 5. Spin time Vs PDMS thickness at 2000 rpm.

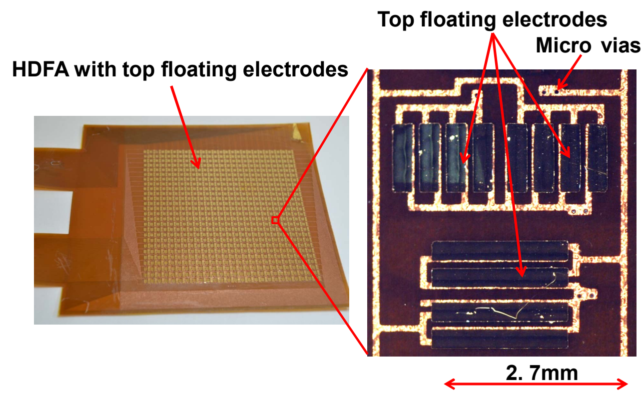

Figure 6. Images of the fabricated HDFA and a close-up view of a sensing cell.

IV. TESTING RESULTS

After the fabrication, HDFAs were integrated with a readout circuit consisting of two custom CMOS switched capacitor ASICs capable of measuring the capacitances of half of the HDFA with a resolution of 13-bits. The details of the circuitry are discussed elsewhere [7].

Nominal unloaded capacitances of X-cell/Y-cell were measured using the readout circuit and found to be 1.25 pF. The measured nominal capacitance is higher than the calculated value due to the presence of additional parasitic and fringing capacitances. Fig. 7 shows a comparison of X-cell-to-Y-cell variation for the previous design [5] and the new HDFA. The new cell experiences a much smaller variation.

The fabricated HDFAs are characterized in a set of experiments categorized into three sections.

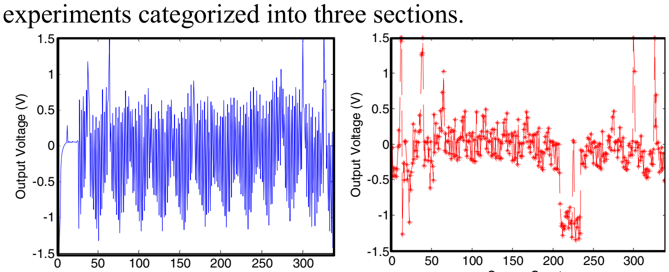

Figure 7. Comparison of unloaded X-cell-to-Y-cell variation of previous design [5] represented in blue to the HDFA represented in red. The new design showed a much lower cell-to-cell variation.

a) Characterization of Individual Cells: Individual cells of the HDFA were interrogated with pre-set values of normal/shear stress applied on them and the corresponding voltage changes are recorded and plotted as shown in Fig. 8 (a) and Fig. 8 (b). After the application of normal stress of 320 kPa (corresponding to the load of an average human), the measured capacitance change is about 0.126 pF which indicates that the PDMS thickness shrunk by 1.56 µm. It can also be inferred from the measurements that the Young's modulus of PDMS is about 2 MPa. When the HDFA is subjected to a shear stress of 115 kPa, the corresponding change in capacitance is 16.25 fF. This indicates a shear modulus of 660 kPa for PDMS.

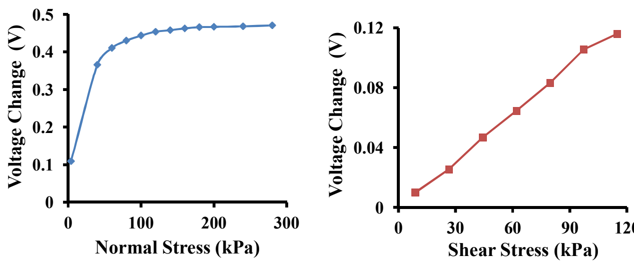

Figure 8. Change in voltage due to various applied normal/shear stresses.

b) Dynamic Contour Pressure Mapping: In order to characterize dynamic pressure mapping using the HDFA, a softball was placed on top of it and rolled randomly by hand. The resulting change in the pressure contours are shown in Fig. 9 (a). The corresponding centroid data of the pressure contours are calculated and displayed in Fig. 9(b).

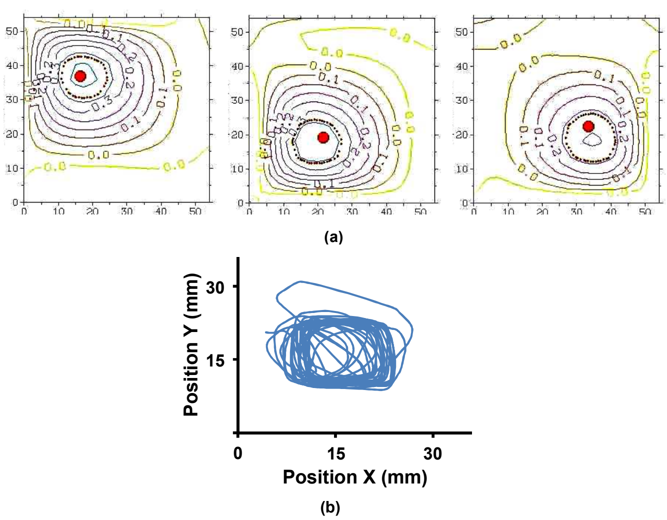

Figure 10. (a) Pressure contours of a 30 mm ball rolling in a circular motion randomly by hand, (b) plot representing the centroid position of the pressure contour of the ball.

c) Measurement of Resolvable Displacement: A soft ball 30 mm in diameter was placed stationary on the HDFA. The pressure centroid position was calculated from the HDFA pressure data. Fig. 11 shows the centroid position versus time determined by 10-point boxcar average of the raw centroid data. The centroid noise band obtained from this plot was 35 µm with RMS noise of 7.54 µm. This resolvable displacement corresponds to a minimum detectable contact line velocity of 38 µm/s (assuming a 200 ms foot ground reaction time).

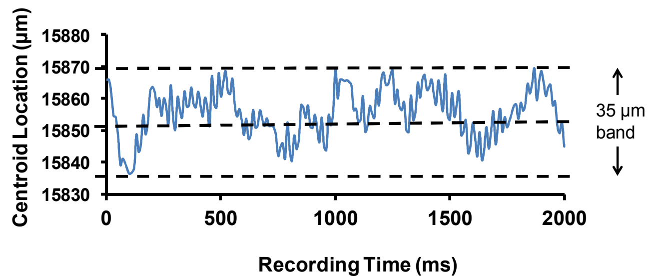

Figure 10. Centroid noise (35 µm) with RMS noise of 7.54 µm.

V. Conclusion

We successfully fabricated a 3-axis HDFA consisting of a modified sensor cell formed using floating electrodes supported by an elastic layer on top of a FPCB substrate. The new design helped reduce the cell-to-cell variation compared to the previous design. The sensing cell in the new design measured only 2.77×2.55 mm^2. The fabricated HDFA compactly packed 2704 capacitors in about 50 cm^2. Each sensing cell consists of multi-finger drive and sense electrodes on the FPCB and floating electrodes placed at an offset on a elastomeric dielectric material spin coated over the FPCB. The fabricated HDFA was successfully characterized. It demonstrated the capability of measuring a resolvable displacement of 35 µm and contact line velocity of 38 µm/s.

References

[1] V. J. Lumelsky, M. S. Shur, and S. Wagner, “Sensitive skin,” IEEE Sensors J., vol. 1, no. 1, pp. 41–51, Jun. 2001.

[2] R. A. Boie, "Capacitive impedance readout tactile image sensor," *Proc. 1984 IEEE International Conference on Robotics and Automation*, vol.1, no., pp. 370- 378, 1984.

[3] D. Johnston, Ping Zhang, J. Hollerbach and S. Jacobsen, "A full tactile sensing suite for dextrous robot hands and use in contact force control," *Proc. 1996 IEEE International Conference on Robotics and Automation*, vol.4, no., pp.3222-3227, 1996.

[4] M. Y. Cheng, C. L. Lin and Y. J. Yang, "Tactile and shear stress sensing array using capacitive mechanisms with floating electrodes," *Proc. IEEE MEMS*, vol., no., pp.228-231, 24-28 Jan. 2010.

[5] R. Surapaneni, Q. Guo, Y. Xie, D. J. Young and C. H. Mastrangelo, " A three-axis high-resolution capacitive tactile imager system based on floating comb electrodes", J. Micromech. Microeng. vol.23, no. 7, pp.5004-5012, 2013.

[6] M. Suster, et al, "Low-Interference Sensing Electronics For High-Resolution Error-Correcting Biomechanical Ground Reaction Sensor Cluster", Proc. IEEE Sensors, pp. 1020-1023, 2010.